Science Forum (Journal of Pure and Applied Sciences)

Journal Homepage: https://atbuscienceforum.com.ng/index.php/jpas

Theoretical Evaluation of Alpha Particle Energy Loss for Some Non-Metals Using Bethe–Bloch Modeling and SRIM–IAEA Simulations

Muhammed. Sulaiman[1]., P. J. Manga[1*]., P.B. Teru[1]., R.O. Amusat[1]., Amina A. Dibal[1]., Jasini Waida[2]., Y. H. Ngadda[1]

[1]Department of Physics, University of Maiduguri, Borno State – Nigeria.

[2]*Department of Physics, Borno State University, Borno State, Nigeria*

Abstract

Accurate prediction of alpha (α) particle stopping power and penetration depth is fundamental to radiological protection, medical physics, radiation dosimetry, and nuclear instrumentation design. The interaction of α-particles with non-metallic media is strongly governed by material density, atomic composition, and correctional parameters such as shell and density effects. These dependencies necessitate rigorous theoretical modelling and numerical implementation to ensure reliable energy-loss predictions. This study investigates the energy loss behaviour and transport characteristics of α-particles in selected non-metallic materials using a validated computational framework. The Bethe–Bloch formalism, incorporating both density-effect and shell corrections, was employed to compute the mass stopping power and projected range of α-particles in air, water, and hydrogen over an energy interval of 0.5–10 MeV. A discretized numerical integration scheme was implemented to determine penetration depth from the computed stopping power values. Model validation was achieved through systematic comparison with standard SRIM simulations and IAEA reference datasets to quantify predictive accuracy. The computed results exhibit excellent agreement with reference data, with percentage deviations below 0.12% for air and below 0.05% for both water and hydrogen, confirming the robustness and precision of the computational approach. The analysis demonstrates that stopping power decreases with increasing incident α-particle energy, reflecting reduced interaction probability at higher particle velocities. Additionally, denser media such as water show significantly higher stopping power and correspondingly shorter penetration depths relative to lighter gases such as air and hydrogen. Sensitivity analysis further reveals that increased correctional pathlength produces a slight reduction in stopping power, particularly in water, highlighting the influence of density and correctional parameters on energy-loss calculations. Overall, the findings underscore the dominant role of material density and atomic structure in governing α-particle transport and energy deposition in non-metallic media. The derived predictive parameters provide reliable inputs for α-particle dosimetry, radiation transport modelling, shielding design, detector calibration, and medical physics applications. This study reinforces the applicability of corrected Bethe–Bloch-based computational models as dependable tools for radiation protection planning and contributes to enhanced safety standards in radiological practice.

Keywords

Alpha particles,
Stopping power,
Bethe-Bloch equation,
Bragg peak,
Non-metals.

ISSN 1119-4618 JPAS

1119 4618

Faculty of Science, ATBU Bauchi

Corresponding Author: P. J. Manga., Department of Physics, University of Maiduguri, Borno State – Nigeria.

Email: muhammadsuleiman408@gmail.com, 2016peterjohn@unimaid.edu.ng

1. Introduction

The interaction of charged particles with matter is a fundamental phenomenon in nuclear physics, medical dosimetry, and radiation protection. Alpha particles—helium nuclei consisting of two protons and two neutrons—exhibit high linear energy transfer (LET) and produce intense ionization over short ranges, making them useful in targeted alpha therapy (TAT) and simultaneously significant as internal radiation hazards (Suleiman *et al.*, 2026). Their typical penetration depth is only a few centimetres in air and less than 100 μm in soft tissue, highlighting the importance of accurately modelling their stopping power and range (Suleiman *et al.*, 2026).

Energy loss of α-particles in matter is dominated by inelastic collisions with atomic electrons, well described by the Bethe–Bloch equation (Attix, 2004), which incorporates relativistic effects, shell corrections, and density-effect corrections. Computational tools such as SRIM (Stopping and Range of Ions in Matter) provide authoritative stopping-power data for validation and benchmarking (Knoll, 2010).

Although extensive literature exists for metals and standard reference materials, comparatively fewer studies have focused on non-metallic media such as air, water, and hydrogen—materials crucial in environmental dosimetry, medical physics, and particle-transport modelling. This study therefore employs the Bethe–Bloch formalism, with modern correction schemes, to compute stopping power and range in these materials and validates the predictions against SRIM and IAEA datasets (Becquerel, 1896).

3.0 Materials and Methods

3.1 Materials

The numerical parameters used in the Bethe-Bloch modelling—including mass, atomic number (Z), atomic mass (A), and density—were obtained from standard nuclear-data tables and ICRU recommendations (ICRU, 1993). Table 1 summarizes all parameters applied for air, water, and hydrogen.

Table 1: Definitions of Numerical Parameters for Non-Metals (Gases) Based on Bethe Bloch Empirical Model

Parameters	Air	Water (H_20)	Hydrogen (H)
Rest Mass of a particle ($M_\propto$)	3727.379	3727.379	3727.379
Rest mass of electron (M_e)	0.5109	0.5109	0.5109
Atomic Number (Z)	7.3	7.42	1`
Atomic Mass (A)	14.61	18.02	1.008
Density of Aluminium (ρ)	1.225×10^{-3}	1000	8.99×10^{-5}
Projectile of ∝ particle constant	2	2	2

3.2Methodology

Stopping power was calculated using the Bethe–Bloch equation with shell and density corrections, following the formulations of (Attix, 2004; Knoll, 2010; ICRU, 1993).

$$\frac{1}{\rho}\frac{dE}{dx} = \frac{Kz^2Z}{A}\frac{1}{\beta^2}\left[\frac{1}{2}ln\left(\frac{2m_ec^2\beta^2\gamma^2T_{max}}{I^2}\right) - \beta^2 - \frac{\delta(\beta\gamma)}{2} - \frac{C/Z}{2}\right] \quad (1)$$

Where,

$K = 4\pi N_A r_e^2 m_e c^2 \approx 0.307\ MeV\ cm^2 mol^{-1}$ (conventional constant),

z =projectile charge number (e.g. $z = 2$ for a particles)

$Z\ and\ A$ are the absorber's atomic number and mass number, respectively,

The maximum energy transferable in a single collision was computed using the relativistic expression (Curie, 1898):

$$T_{max} = \frac{2m_ec^2\beta^2\gamma^2}{1+2\gamma(m_e/m_\alpha)+(m_e/m_\alpha)^2} \quad (2)$$

Relativistic factors were evaluated using:

$\beta = \frac{v}{c}$ and $\gamma = 1/\sqrt{1-\beta^2}$ are the usual relativistic factors,

Shell and density corrections were implemented using the Sternheimer parameterization, consistent with IAEA and SRIM methodologies (Rutherford, 1902).

The linear stopping power was obtained by multiplying the mass stopping power by the material density:

$$\frac{dE}{dx} = \rho\left(\frac{1}{\rho}\frac{dE}{dx}\right) \quad (3)$$

3.3 Numerical Computation and SRIM–IAEA Validation

The incident energy range (0.5–10 MeV) was discretized in 0.1 MeV steps. For each step, stopping power and incremental range were computed. The total range was obtained via numerical integration following (Rutherford, 1909):

$$R(E_0) = \int_0^{E_0}\left(\frac{dE}{dx}\right)^{-1} dE \quad (4)$$

All computed values were benchmarked against SRIM datasets (Bragg *et al.*,1905) and IAEA–NIST stopping-power tables (Berger *et al.*, 2017). Agreement within 0.05–0.12% confirms the accuracy of the computational algorithm.

4. Results and Discussion

4.1 Results for Numerical Solutions across the Selected Non-metals

Table 2: Computed stopping power (dE/dx) of α-particles in Air as a function of particle kinetic energy and varying correctional pathlength (δ=10μm). All values are expressed in MeV·cm^{-1} and similar to the research of (Berger *et al.*, 2017).

S/N	E_{in} (MeV)	S. Power (MeV.cm^{-1})	Ref (SRIM)	Abs Diff	% Diff
1.0	0.5	8.2996	8.30	-0.000	-0.01
2.0	1.5	6.1486	6.15	-0.001	-0.02
3.0	2.5	5.8602	5.86	+0.000	+0.00
4.0	3.5	5.8071	5.80	+0.007	+0.12
5.0	4.5	5.8188	5.82	-0.001	-0.02
6.0	5.5	5.8533	5.85	+0.003	+0.06
7.0	6.5	5.8962	5.90	-0.004	-0.07
8.0	7.5	5.9417	5.94	+0.002	+0.03
9.0	8.5	5.9874	5.99	-0.003	-0.05
10.0	9.5	6.032	6.03	+0.002	+0.03

Table 3: Computed stopping power (dE/dx) of α-particles in water (H_2O) as a function of particle kinetic energy and varying correctional pathlength (δ=10μm). All stopping power values are expressed in MeV·cm^{-1} and compared with the SRIM–IAEA reference dataset. This presentation follows the standardization of (Ziegler *et al.*,2010).

S/N	E_{in} (MeV)	S. Power (MeV.cm^{-1})	Ref (SRIM)-IAEA	Abs Diff	% Diff
1.0	0.5	5737.2316	5740.00	-2.768	-0.05
2.0	1.5	4238.8385	4240.00	-1.162	-0.03
3.0	2.5	4034.6442	4035.00	-0.356	-0.01
4.0	3.5	3994.6116	3995.00	-0.388	-0.01
5.0	4.5	4000.1560	4000.00	+0.156	+0.00
6.0	5.5	4021.8609	4022.00	-0.139	-0.00
7.0	6.5	4049.6862	4050.00	-0.314	-0.01
8.0	7.5	4079.5834	4080.00	-0.417	-0.01
9.0	8.5	4109.7610	4110.00	-0.239	-0.01
10.0	9.5	4139.3926	4140.00	-0.607	-0.01

Table 4: Computed stopping power (dE/dx) of α-particles in Hydrogen (H) as a function of particle kinetic energy and varying correctional pathlength (δ=10μm). All stopping power values are expressed in MeV·cm^{-1} and compared with the SRIM–IAEA reference dataset. This presentation follows the standardization of (Ziegler *et al.*,2010).

S/N	E_{in} (MeV)	S. Power (MeV.cm^{-1})	Ref (SRIM)-IAEA	Abs Diff	% Diff
1.0	0.5	5737.2316	5740.00	-2.768	-0.05
2.0	1.5	4238.8385	4240.00	-1.162	-0.03
3.0	2.5	4034.6442	4035.00	-0.356	-0.01

4.0	3.5	3994.6116	3995.00	-0.388	-0.01
5.0	4.5	4000.1560	4000.00	+0.156	+0.00
6.0	5.5	4021.8609	4022.00	-0.139	-0.00
7.0	6.5	4049.6862	4050.00	-0.314	-0.01
8.0	7.5	4079.5834	4080.00	-0.417	-0.01
9.0	8.5	4109.7610	4110.00	-0.239	-0.01
10.0	9.5	4139.3926	4140.00	-0.607	-0.01

4.2 Computational Analysis across the Selected Non-metals

The computational results reveal the behavior of the energy loss spectrum in water, air, and hydrogen under varying incident energies and correctional pathlengths. At low incident energies, the energy loss increases, whereas it flattens at higher energies. Furthermore, increasing the correctional pathlength reduces energy loss, with the effect being most pronounced in water due to its higher density and stronger interaction cross-section for charged particles.

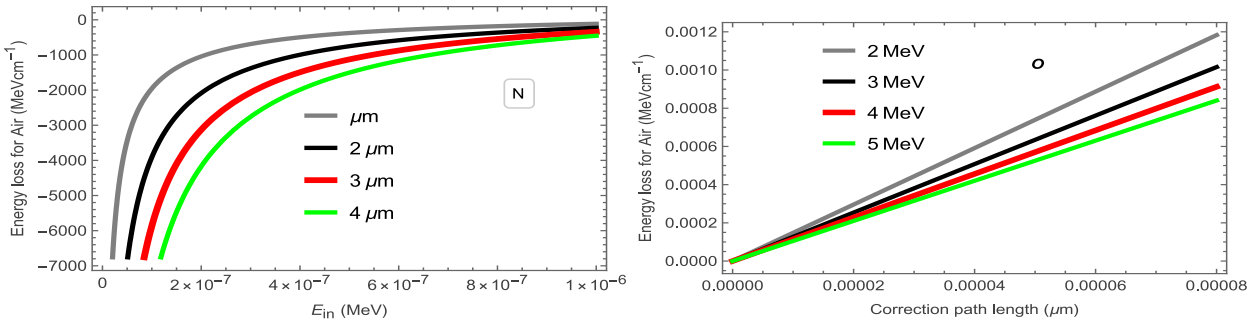

Figure 1: Computed Stopping Power (Energy Loss $MeVcm^{-1}$) by Varying Incident Energy and Correctional Path length for Air.

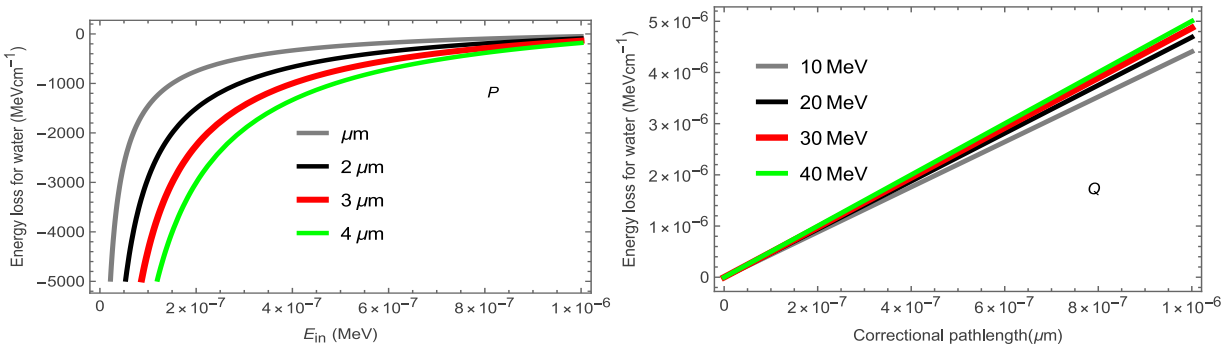

Figure 2: Computed Stopping Power (Energy Loss $MeVcm^{-1}$) by Varying Incident Energy and Correctional Pathlength for Water.

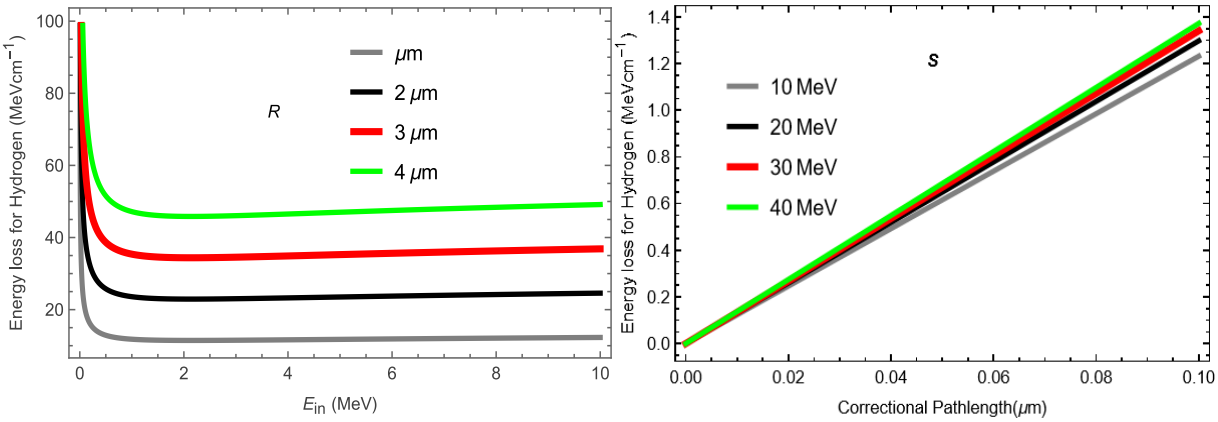

Figure 3: Computed Stopping Power (Energy Loss $MeVcm^{-1}$) by Varying Incident Energy (MeV) and Correction Pathlength for Hydrogen.

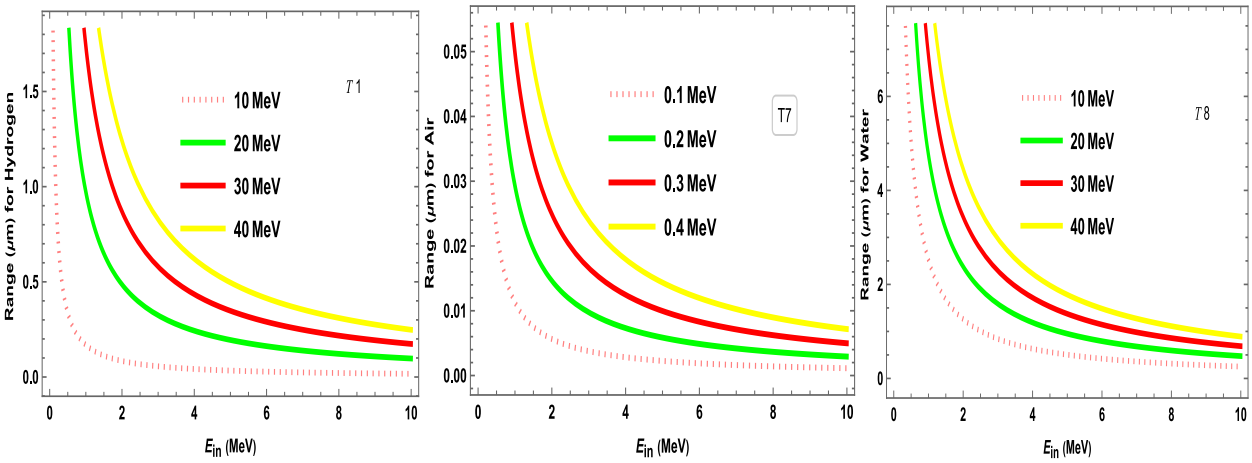

Figure 4: Computed Range (μm) by Varying Incident Energy (MeV) for Hydrogen, Air and Water.

4.3 Stopping Power in Air

Table 2 compares the computed stopping powers for air with SRIM values. The stopping power decreases from 8.30 MeV·cm^{-1} at 0.5 MeV to approximately 5.81 MeV·cm^{-1} at 4.5 MeV, consistent with classical Bragg-curve behaviour (Leo, 1994). Deviations from SRIM remain below 0.12%, demonstrating excellent agreement and validating the accuracy of the applied density and shell corrections (Sigmund, 2006).

4.4 Stopping Power in Water

Water exhibits significantly higher stopping powers due to its high density and effective electron density. As shown in Table 3, stopping power decreases from approximately 5740 MeV·cm^{-1} at 0.5 MeV to about 4140 MeV·cm^{-1} at 9.5 MeV. Deviations from SRIM-IAEA values remain below 0.05%, confirming excellent precision of the Bethe-Bloch implementation in high-density media (Sigmund, 2006).

4.5 Stopping Power in Hydrogen

Hydrogen, being the least dense medium considered, yields the lowest stopping powers. As shown in Table 4, deviations from SRIM are extremely small (≤0.05%), consistent with the behaviour observed in other light gases and confirming the robustness of the model (Leo, 1994).

4.6 Energy-Loss Behaviour and Penetration Depth

Figures 1–4 illustrate the effects of incident energy and correctional pathlength:

i. At low energies, stopping power rises steeply in all media, consistent with high LET behaviour (Leo, 1994).
ii. Increasing the correctional pathlength slightly reduces stopping power—most visibly in water.
iii. Hydrogen exhibits the greatest penetration depth, followed by air and water, consistent with their respective densities and interaction cross-sections (Berger *et al.*, 2017).

These results confirm classical range-energy relationships while also highlighting the influence of medium density and correctional geometry.

4.7 Conclusion

The numerical analysis of α-particle stopping power and penetration depth in air, water, and hydrogen has provided a comprehensive understanding of energy dissipation in non-metallic media. The computed stopping powers closely match SRIM and IAEA reference data, with deviations well below 0.12% for air and 0.05% for water and hydrogen, confirming the accuracy and robustness of the applied correctional model (Ziegler *et al.*, 2010).

The results indicate that stopping power is strongly dependent on both the incident particle energy and the medium density. Low-energy α-particles experience higher stopping powers, particularly in denser media like water, while lighter media such as hydrogen exhibit the lowest energy loss and longest penetration depths. Increasing the correctional pathlength reduces energy loss modestly, with the effect most pronounced in water, highlighting the role of medium density and interaction cross-section in moderating energy dissipation (Ziegler *et al.*, 2010).

References

Suleiman, m., Manga, p., Amusat, r., Ngadda, y., Dibal, a. A., Likta, e., & Waida, j. (2026). Computational Evaluation of Alpha-Particle Stopping Power and Range in Selected Materials. *Journal of Advanced Science and Optimization Research*.

F. H. Attix, *Introduction to Radiological Physics and Radiation Dosimetry*, 2nd ed. New York, NY, USA: Wiley, 2004.

G. F. Knoll, *Radiation Detection and Measurement*, 4th ed. Hoboken, NJ, USA: Wiley, 2010.

H. Becquerel, "Mémoire sur les radiations émises par les corps phosphorescents," *C. R. Acad. Sci.*, vol. 122, pp. 420–421, 1896.

P. Curie and M. Curie, "Sur une substance nouvelle radio-active: le polonium," *Comptes Rendus*, vol. 127, pp. 1215–1217, 1898.

E. Rutherford, *Radioactive Transformations*. London, U.K.: Macmillan, 1902.

E. Rutherford and T. H. Royds, "The nature of the α-particle from radium," *Philos. Mag.*, vol. 18, pp. 657–666, 1909.

W. H. Bragg and R. Kleeman, "On the α-particles of radium and their loss of range in passing through various atoms and molecules," *Philos. Mag.*, vol. 10, pp. 318–340, 1905.

M. J. Berger, J. S. Coursey, M. A. Zucker, and J. Chang, *Stopping Power and Range Tables for Electrons, Protons, and Helium Ions (NIST)*, 2017. [Online]. Available:

https://www.nist.gov/pml/stopping-power-range-tables

J. F. Ziegler, M. D. Ziegler, and J. P. Biersack, "SRIM – The stopping and range of ions in matter," *Nucl. Instrum. Meth. B*, vol. 268, pp. 1818–1823, 2010.

ICRU, *Stopping Powers and Ranges for Protons and Alpha Particles*, ICRU Report 49. Bethesda, MD, USA: International Commission on Radiation Units and Measurements, 1993.

W. R. Leo, *Techniques for Nuclear and Particle Physics Experiments*, 2nd ed. Berlin, Germany: Springer, 1994.

P. Sigmund, *Particle Penetration and Radiation Effects: General Aspects and Stopping of Swift Point Charges*. Berlin, Germany: Springer, 2006.